Substituting scheme for nonlinear couplers: A group approach

Jaromír Fiurášek[1,2] and Jan Peřina[2]
[1]*Department of Chemical Physics, The Weizmann Institute of Science, 76100 Rehovot, Israel*
[2]*Department of Optics, Palacký University, 17. listopadu 50, 772 07 Olomouc, Czech Republic*
(Received 18 January 2000; published 11 August 2000)

We consider a substituting scheme for nonlinear optical couplers operating by means of degenerate parametric down-conversion with strong coherent pumping. The proposed scheme, which provides the same unitary input-output transformation as the original coupler, consists of simple linear and nonlinear optical devices: beam splitter and optical parametric amplifiers. Using a group-theoretical approach, we find analytical formulas for parameters of these optical elements. The scheme allows us to get a better insight into the coupler behavior, because the complex dynamics of the coupler is transformed into a sequence of simpler evolutions governed by the beam splitter and parametric amplifiers, whose properties are well known and understood. We demonstrate that various dynamical regimes of the coupler are clearly reflected by the substituting device.

PACS number(s): 42.50.−p, 42.65.Wi

I. INTRODUCTION

Recently, increasing attention has been devoted to nonlinear optical couplers. The optical coupler is a device formed from two closely lying parallel optical waveguides, whose guided modes are thus coupled by means of evanescent waves. In a nonlinear coupler, some nonlinear optical process takes place in one or both waveguides. Nonlinear couplers can be employed in telecommunication systems as all-optical switchers [1,2] and they can serve in optical data processing as logical gates [3].

The generation and propagation of nonclassical light in nonlinear couplers have been studied extensively. The assumed nonlinear processes included degenerate [4–6] and nondegenerate [2,7] parametric down-conversion, Kerr nonlinearity [8,9], and Raman and Brillouin scattering [10–12]. The propagation of Schrödinger-cat states through the coupler has been studied [13] and the quantum phase properties of optical modes propagating in couplers have been investigated [14,15]. For a review, see [16].

In these theoretical studies, both codirectional and contradirectional couplers have been considered. Recently, the contradirectional coupler has been realized experimentally [17,18]. The correct quantum description of light propagation in the contradirectional coupler has been a matter of some discussion. It was shown that a unitary input-output transformation can be found for couplers described by quadratic Hamiltonians [19]. However, the evolution of the field inside the contradirectional coupler is not unitary. A broad class of contradirectional devices can be simulated by codirectional ones provided that parameters of codirectional devices are suitably chosen [20]. A typical feature of the simulating device proposed in [20] is that its linear and nonlinear coupling parameters change with distance.

A broad class of nonlinear couplers can be characterized by quadratic Hamiltonians. This is usually achieved by making an assumption of strong coherent laser pumping of some modes. The unitary evolution operator corresponding to the N-mode quadratic Hamiltonian represents a transformation belonging to a symplectic group $Sp(2N,R)$. Various properties of these transformations have been studied [21–25]. There are basically two types of transformations in $Sp(2N,R)$. Those conserving the total photon number form a compact group $U(N)$. For example, an ideal lossless beam splitter realizes transformation from the group $U(2)$ [26]. The remaining transformations do not conserve the total photon number and they are called squeeze transformations. It is worth noting that a class of optical fields with Gaussian quasidistributions is invariant under symplectic transformations. Particularly, any pure Gaussian state can be constructed from the coherent state with the use of appropriate symplectic transformation.

In this paper, we investigate the symplectic transformations describing the operation of nonlinear couplers. To achieve some insight into the properties of this transformation, we decompose it into a product of simple transformations belonging to one-parametric subgroups of $Sp(2N,R)$. This factorization has a simple physical meaning: the coupler is replaced by a sequence of simpler linear and nonlinear optical devices, namely beam splitters and optical parametric amplifiers. Thus we construct a substituting scheme for the coupler and study its properties. To provide a complete picture, we also briefly discuss the generation of nonclassical light in the coupler.

The paper is organized as follows. In Sec. II, a substituting scheme for the codirectional coupler is introduced and the analytical formulas for its parameters are obtained. The generation of nonclassical light in the coupler is discussed in Sec. III. In Sec. IV, the numerical results and discussion for the codirectional coupler are provided. A similar treatment of the contradirectional coupler can be found in Sec. V. Finally, Sec. VI contains conclusions.

II. SUBSTITUTING SCHEME FOR THE CODIRECTIONAL COUPLER

A. Nonlinear coupler and group $Sp(4,R)$

The nonlinear coupler operating by means of degenerate parametric down-conversion with strong coherent pumping is depicted in Fig. 1. The two guided beams propagating

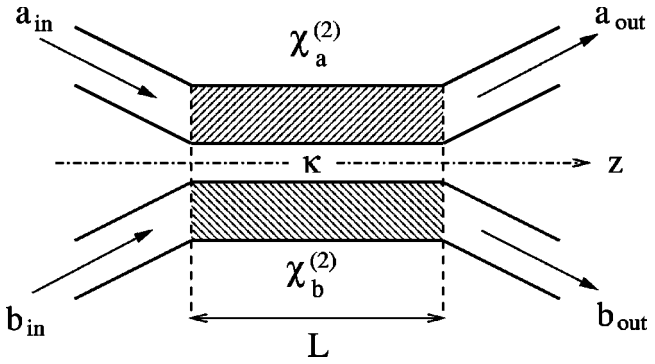

FIG. 1. Sketch of the nonlinear codirectional coupler formed from two waveguides characterized by quadratic susceptibilities $\chi_a^{(2)}$ and $\chi_b^{(2)}$, respectively. κ denotes a linear coupling constant between the two waveguides; L is the coupler's length.

through the coupler are treated as single-mode fields. This coupler can be described by the interaction momentum operator [4]

$$G=\hbar g_a a^2+\hbar g_b b^2+\hbar\kappa a b^\dagger+\text{H.c.}, \tag{1}$$

where a and b are the annihilation operators of the modes propagating in the first and second waveguides, respectively, and H.c. denotes the Hermitian conjugate term. We use momentum operator G rather than Hamiltonian H. We do not consider dispersion and assume that propagation constants of modes a and b are the same, $\beta_a=\beta_b$. Thus the momentum operator G is proportional to the Hamiltonian H, $H=cG$, c is the velocity of light beams propagating in the coupler, and the descriptions based on G and H are equivalent. It is more convenient to use G as we deal with propagating beams. The Heisenberg equations for the operators a and b in the interaction picture follow from $i\hbar dX/dz=[G,X]$ (X denotes an arbitrary operator),

$$\begin{aligned}\frac{da}{dz}&=2ig_a a^\dagger+i\kappa b,\\ \frac{db}{dz}&=2ig_b b^\dagger+i\kappa a.\end{aligned} \tag{2}$$

The propagation distance z can be considered as a convenient measure of the interaction time $t=z/c$. Nonlinear coupling constants $g_a\propto\chi_a^{(2)}\alpha$ and $g_b\propto\chi_b^{(2)}\beta$ characterize the strength of degenerate parametric down-conversion in the first and second waveguides, respectively. $\chi_j^{(2)}$ denotes the quadratic susceptibility of the core of the jth waveguide, and α and β are amplitudes of strong coherent laser pumping of the corresponding second-harmonic modes. The linear coupling constant κ describes the mutual coupling between modes a and b in the coupler. The assumption of strong coherent laser pumping simplifies the analysis considerably because the momentum operator G belongs to a class of quadratic operators. The Heisenberg equations (2) are linear and can be easily solved. The momentum operator G is a generator of a one-parametric subgroup of the symplectic group $Sp(4,R)$. This group consists of all transformations generated by Hermitian quadratic operators constructed from operators a, $a^\dagger$, b, and $b^\dagger$. The group $Sp(4,R)$ has altogether ten generators, which can be connected with various physical devices, such as beam splitters, phase shifters, degenerate optical parametric amplifiers (DOPA), and nondegenerate optical parametric amplifiers (NDOPA) [21,26].

In this paper, we replace the nonlinear coupler by a sequence of simpler devices: beam splitters, DOPA, and NDOPA. In other words, we construct a substituting scheme for the nonlinear coupler and study the dependence of its properties on the propagation distance z and the coupling parameters g_a, g_b, and κ. We show that various dynamical regimes of the coupler are clearly reflected by the substituting scheme. We assume that all coupling constants in momentum operator (1) are real. This assumption allows us to work in a four-parametric subgroup of group $Sp(4,R)$. In physical terms, we will need only four devices to represent our nonlinear coupler.

Let us introduce the operators

$$\begin{aligned}U&=a^{\dagger 2}+a^2,\\ V&=b^{\dagger 2}+b^2,\\ W&=a^\dagger b+a b^\dagger,\\ Y&=iab-ia^\dagger b^\dagger.\end{aligned} \tag{3}$$

U and V are generators of single-mode squeeze operators

$$\mathcal{U}_a(u)=\exp(iuU),\quad \mathcal{V}_b(v)=\exp(ivV), \tag{4}$$

which can be realized by DOPAs. W is a generator of linear mixing which can be achieved by the ideal lossless beam splitter BS and described by the operator

$$\mathcal{W}_{ab}(w)=\exp(iwW). \tag{5}$$

Finally, the operator Y generates two-mode squeezing and NDOPA can be used to implement this transformation. The corresponding two-mode squeeze operator reads

$$\mathcal{Y}_{ab}(y)=\exp(iyY). \tag{6}$$

Commutation relations for operators (3) will be important in the following calculations. They read

$$\begin{aligned}&[U,V]=0,\quad [V,W]=-2iY,\\ &[U,W]=-2iY,\quad [V,Y]=-2iW,\\ &[U,Y]=-2iW,\quad [W,Y]=-i(U+V).\end{aligned} \tag{7}$$

With the help of the operators (3), we can rewrite G as

$$G=\hbar(g_a U+g_b V+\kappa W). \tag{8}$$

Although only operators U, V, and W are present in the momentum operator G, we need also Y to form a closed Lie commutator algebra (7).

The unitary evolution operator $\mathcal{I}(z)$ is generated by the momentum operator (1),

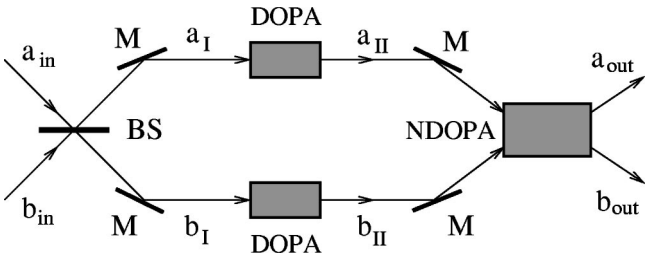

FIG. 2. Substituting scheme for nonlinear coupler. The coupler is replaced by a sequence of beam splitter BS, two degenerate parametric amplifiers DOPA, and one nondegenerate parametric amplifier NDOPA. *M* denotes auxiliary mirrors.

$$\mathcal{I}(z)=\exp(iGz/\hbar). \tag{9}$$

We would like to decompose this unitary operator into a product of simpler unitary operators as follows:

$$\mathcal{I}(z)=\mathcal{Y}_{ab}(y)\mathcal{U}_a(u)\mathcal{V}_b(v)\mathcal{W}_{ab}(w). \tag{10}$$

The right-hand side represents a sequence of linear mixing operator, single-mode squeeze operators, and two-mode squeeze operator. A physical device reflecting this factorization is shown in Fig. 2. The modes *a* and *b* are mixed at the beam splitter BS, each mode is then squeezed in DOPA, and finally both modes are mixed in NDOPA. The scheme depicted in Fig. 2 is similar to the nonlinear Mach-Zehnder interferometer discussed in [27]. However, the second beam splitter of the interferometer is replaced by NDOPA. Note also that a different type of nonlinear Mach-Zehnder interferometer containing Kerr media in its arms was analyzed in [28].

The factorization given in Eq. (10) is only one of many possibilities. Since the operators (3) do not commute, various orderings on the right-hand side of Eq. (10) represent different substituting schemes. Inserting the explicit expressions (4), (5), (6), and (9) into Eq. (10), we can rewrite this formula as

$$e^{iGz/\hbar}=e^{iy(z)Y}e^{iu(z)U}e^{iv(z)V}e^{iw(z)W}. \tag{11}$$

The substituting scheme is fully characterized by the parameters

$$u(z),\ v(z),\ w(z),\ \text{and}\ y(z), \tag{12}$$

which are functions of the propagation length z and which also depend on the coupling constants g_a, g_b, and κ. In particular, $z=L$. The parameters (12) will be the main tool in our investigation of the coupler operation.

We can use two different equivalent approaches to find the parameters (12). They can be determined as a solution of the system of nonlinear differential equations or by solving the system of nonlinear algebraic equations.

B. Differential equation approach

In order to derive differential equations for the factorization parameters (12), we employ a general procedure which was first proposed in Ref. [29]. The main idea is to differentiate Eq. (11) and then to use commutation rules (7) to simplify the resulting expression.

We can simplify the calculations by noting that the operator $U_-=U-V$ commutes with all four operators U, V, W, and Y. We introduce the operator $U_+=U+V$, new parameters $u_\pm=(u\pm v)/2$, and coupling constants $g_\pm=(g_a\pm g_b)/2$, which allows us to write

$$e^{iu(z)U}e^{iv(z)V}=e^{iu_+(z)U_+}e^{iu_-(z)U_-}. \tag{13}$$

The nonzero commutators are

$$\begin{aligned}[U_+,W]&=-4iY,\\ [U_+,Y]&=-4iW,\\ [W,Y]&=-iU_+.\end{aligned} \tag{14}$$

Now we substitute Eq. (13) into Eq. (11) and differentiate:

$$\begin{aligned}\hbar^{-1}Ge^{iGz/\hbar}=&\,y'Ye^{iyY}e^{iu_+U_+}e^{iu_-U_-}e^{iwW}\\ &+e^{iyY}u'_+U_+e^{iu_+U_+}e^{iu_-U_-}e^{iwW}\\ &+e^{iyY}e^{iu_+U_+}u'_-U_-e^{iu_-U_-}e^{iwW}\\ &+e^{iyY}e^{iu_+U_+}e^{iu_-U_-}w'We^{iwW},\end{aligned} \tag{15}$$

where the primes denote derivatives with respect to z, and the z dependence of the parameters $u_\pm$, w, and y is not explicitly displayed for typographical simplicity. In the next step, Eq. (15) is multiplied by the inverse operator $\exp(-iGz/\hbar)$. Due to the operator nature of Eq. (15), we have to distinguish multiplications from the left and from the right. These two possibilities result in two distinct differential equations for parameters (12). Nevertheless, these two sets of equations are equivalent and give the same results for the initial conditions

$$u(0)=v(0)=w(0)=y(0)=0. \tag{16}$$

The operator $\exp(-iGz/\hbar)$ is expressed as an inversion of the right-hand side of Eq. (11) and the following relations are used to simplify Eq. (15):

$$\begin{aligned}e^{isU_+}We^{-isU_+}&=W\cosh(4s)+Y\sinh(4s),\\ e^{isU_+}Ye^{-isU_+}&=Y\cosh(4s)+W\sinh(4s),\\ e^{isW}U_+e^{-isW}&=U_+\cos(2s)-2Y\sin(2s),\\ e^{isW}Ye^{-isW}&=Y\cos(2s)+\frac{1}{2}U_+\sin(2s),\\ e^{isY}U_+e^{-isY}&=U_+\cosh(2s)-2W\sinh(2s),\\ e^{isY}We^{-isY}&=W\cosh(2s)-\frac{1}{2}U_+\sinh(2s),\end{aligned} \tag{17}$$

where s is an arbitrary real number. A proof of these formulas is very simple. We prove the first one, the others can be

verified in the same way. We consider the left-hand side of the first formula in Eq. (17) as a function of s and calculate its derivatives,

$$f(s)=e^{isU_+}We^{-isU_+},$$

$$f'(s)=ie^{isU_+}[U_+,W]e^{-isU_+}=4e^{isU_+}Ye^{-isU_+}, \quad (18)$$

$$f''(s)=4ie^{isU_+}[U_+,Y]e^{-isU_+}=16e^{isU_+}We^{-isU_+},$$

where we have made use of the commutation rules (14). Comparing the first and third lines in Eq. (18), we find the differential equation for $f(s)$,

$$f''(s)=16f(s), \quad (19)$$

where the prime means the derivative. Solving this equation with appropriate initial conditions $f(0)=W$ and $f'(0)=4Y$, we immediately obtain

$$f(s)=W\cosh(4s)+Y\sinh(4s), \quad (20)$$

and hence we have derived the first formula in Eqs. (17).

Let us first consider multiplication of Eq. (15) by $\exp(-iGz/\hbar)$ from the right. To give an example, we explicitly deal with the fourth line in Eq. (15). Recalling that U_- commutes with all operators and applying repeatedly the relations (17), we find

$$e^{iyY}e^{iu_+U_+}e^{iu_-U_-}w'We^{-iu_-U_-}e^{-iu_+U_+}e^{-iyY}$$
$$=w'\left[-\frac{1}{2}U_+\sinh(2y)\cosh(4u_+)\right.$$
$$\left.+W\cosh(2y)\cosh(4u_+)+Y\sinh(4u_+)\right]. \quad (21)$$

The same exercise is repeated with the first three lines in Eq. (15). Introducing the explicit form (8) of the momentum operator G and comparing coefficients standing with the operators $U_\pm$, W, and Y on the left- and right-hand sides of Eq. (15), we obtain four differential equations. Since U_- commutes with all operators, the equation for u_- separates, $u'_-=g_-$. A trivial integration yields

$$u(z)-v(z)=(g_a-g_b)z. \quad (22)$$

The remaining three coupled equations can conveniently be written in the matrix form

$$\mathbf{N}_{\rm right}\frac{d\mathbf{P}}{dz}=\mathbf{C}, \quad (23)$$

where

$$\mathbf{N}_{\rm right}=\begin{pmatrix}\cosh(2y) & -\frac{1}{2}\cosh(4u_+)\sinh(2y) & 0\\ -2\sinh(2y) & \cosh(4u_+)\cosh(2y) & 0\\ 0 & \sinh(4u_+) & 1\end{pmatrix}$$

and

$$\mathbf{P}=\begin{pmatrix}u_+\\ w\\ y\end{pmatrix}, \quad \mathbf{C}=\begin{pmatrix}g_+\\ \kappa\\ 0\end{pmatrix}. \quad (24)$$

Alternatively, multiplying Eq. (15) by $\exp(-iGz/\hbar)$ from the left, we arrive at

$$\mathbf{N}_{\rm left}\frac{d\mathbf{P}}{dz}=\mathbf{C}, \quad (25)$$

where

$$\mathbf{N}_{\rm left}=\begin{pmatrix}\cos(2w) & 0 & -\frac{1}{2}\cosh(4u_+)\sin(2w)\\ 0 & 1 & -\sinh(4u_+)\\ 2\sin(2w) & 0 & \cosh(4u_+)\cos(2w)\end{pmatrix},$$

and Eq. (22) remains unchanged. The existence of two distinct systems of differential equations will become useful later when we investigate the asymptotic behavior of their solution.

C. Group algebraic approach

From the group-theoretical point of view, the factorization (10) states that the group element $\exp(iGz/\hbar)$ is a composition of four other group elements, each of them being a member of certain one-parametric subgroup of $Sp(4,R)$. If we know the group composition rule, we are able to obtain a set of algebraic equations connecting $u(z)$, $v(z)$, $w(z)$, and $y(z)$ with g_az, g_bz, and κz. This can be achieved in the Heisenberg representation. The vector

$$\mathbf{A}=\begin{pmatrix}a\\ a^\dagger\\ b\\ b^\dagger\end{pmatrix} \quad (26)$$

is introduced and each group element is represented by a 4×4 matrix $\mathbf{M}$. Any quadratic Hermitian operator X can be associated with the matrix $\mathbf{M}_X$ as follows:

$$\exp(-iXz)\mathbf{A}\exp(iXz)=\mathbf{M}_X(z)\mathbf{A}. \quad (27)$$

Particularly, we have

$$\mathbf{M}_U(u)=\begin{pmatrix}\cosh(2u) & i\sinh(2u) & 0 & 0\\ -i\sinh(2u) & \cosh(2u) & 0 & 0\\ 0 & 0 & 1 & 0\\ 0 & 0 & 0 & 1\end{pmatrix}, \quad (28)$$

$$\mathbf{M}_V(v)=\begin{pmatrix}1 & 0 & 0 & 0\\ 0 & 1 & 0 & 0\\ 0 & 0 & \cosh(2v) & i\sinh(2v)\\ 0 & 0 & -i\sinh(2v) & \cosh(2v)\end{pmatrix}, \quad (29)$$

$$\mathbf{M}_W(w)=\begin{pmatrix} \cos w & 0 & i\sin w & 0 \\ 0 & \cos w & 0 & -i\sin w \\ i\sin w & 0 & \cos w & 0 \\ 0 & -i\sin w & 0 & \cos w \end{pmatrix}, \tag{30}$$

and

$$\mathbf{M}_Y(y)=\begin{pmatrix} \cosh y & 0 & 0 & \sinh y \\ 0 & \cosh y & \sinh y & 0 \\ 0 & \sinh y & \cosh y & 0 \\ \sinh y & 0 & 0 & \cosh y \end{pmatrix}. \tag{31}$$

For the operator $G/\hbar$ we can write

$$\mathbf{M}_G(z)=\exp(i\mathbf{F}z), \tag{32}$$

where $\mathbf{F}$ is the 4×4 matrix,

$$\mathbf{F}=\begin{pmatrix} 0 & 2g_a & \kappa & 0 \\ -2g_a & 0 & 0 & -\kappa \\ \kappa & 0 & 0 & 2g_b \\ 0 & -\kappa & -2g_b & 0 \end{pmatrix}. \tag{33}$$

Explicit expressions for elements of matrix $\mathbf{M}_G(z)$ can be found in papers where Heisenberg equations (2) were solved using the Laplace transform technique [4,6]. The eigenvalues of matrix $i\mathbf{F}$ determine the dynamics of the codirectional coupler. They read

$$\lambda_j=\pm(g_a-g_b)\pm[(g_a+g_b)^2-\kappa^2]^{1/2}; \tag{34}$$

all four combinations of signs must be taken into account. Real parts of λ_j give the speed of exponential amplification and imaginary parts yield the frequency of oscillations.

We can distinguish two different dynamical regimes:

(i) $|g_a+g_b|<|\kappa|$, the linear coupling is dominant, the coupler operates below threshold, eigenvalues are complex;

(ii) $|g_a+g_b|>|\kappa|$, the nonlinear interaction dominates, the coupler operates above threshold, all eigenvalues are real. There are also two important specific cases:

(iii) $g_a=g_b=g$, $2|g|<|\kappa|$, all four eigenvalues are purely imaginary, $\lambda_j=\pm i[\kappa^2-4g^2]^{1/2}$;

(iv) $g_a=-g_b=g$, the eigenvalues are $\lambda_j=\pm2g\pm i\kappa$.

We return to these regimes in the discussion in Sec. IV.

With the help of the above matrices, Eq. (11) can be rewritten into

$$\mathbf{M}_G(z)=\mathbf{M}_Y(y)\mathbf{M}_U(u)\mathbf{M}_V(v)\mathbf{M}_W(w). \tag{35}$$

This establishes a system of nonlinear algebraic equations for $u(z)$, $v(z)$, $w(z)$, and $y(z)$. Though it might seem that the system is overdetermined because the matrices have 16 elements, this is not the case. Matrices on the left- and right-hand sides have such a special structure that the factorization (35) yields only four independent equations.

In order to find an analytical solution of Eqs. (35), we consider the input two-mode coherent state $|\xi_a\rangle|\xi_b\rangle$ propagating through the substituting device. After mixing at the beam splitter, the complex amplitudes ξ_a and ξ_b are changed but the modes a_I and b_I remain in coherent states. Then each mode propagates through the parametric amplifier. At the outputs of DOPAs, modes a_{II} and b_{II} are in single-mode squeezed states, but they are not correlated. The correlation between a and b originates in NDOPA, which yields the outputs $a_{\rm out}$ and $b_{\rm out}$. The output state is a pure Gaussian state. Any Gaussian state is fully determined by the coherent components (complex amplitudes) $\xi_a=\langle a\rangle$, $\xi_b=\langle b\rangle$, and by the correlation matrix

$$\mathbf{S}=-\begin{pmatrix} -(B_a+\frac{1}{2}) & C_a & \overline{D}^*_{ab} & D_{ab} \\ C^*_a & -(B_a+\frac{1}{2}) & D^*_{ab} & \overline{D}_{ab} \\ \overline{D}_{ab} & D_{ab} & -(B_b+\frac{1}{2}) & C_b \\ D^*_{ab} & \overline{D}^*_{ab} & C^*_b & -(B_b+\frac{1}{2}) \end{pmatrix}, \tag{36}$$

the elements of which are the noise parameters

$$\begin{aligned} B_a&=\langle\Delta a^\dagger\Delta a\rangle, \quad C_a=\langle(\Delta a)^2\rangle, \\ B_b&=\langle\Delta b^\dagger\Delta b\rangle, \quad C_b=\langle(\Delta b)^2\rangle, \\ \overline{D}_{ab}&=-\langle\Delta a^\dagger\Delta b\rangle, \quad D_{ab}=\langle\Delta a\Delta b\rangle, \end{aligned} \tag{37}$$

where $\Delta a=a-\langle a\rangle$ and $\Delta b=b-\langle b\rangle$. The matrix $\mathbf{S}$ has complex elements. Some authors prefer to use real correlation matrix elements which are formed by correlations between quadratures p_a, q_a, p_b, and q_b. The relation between these two formalisms is given by a simple unitary transformation [23]. It was shown in [24] that the correlation matrix of any Gaussian state can be diagonalized by a sequence of canonical transformations. We adopt this approach here to find analytical expressions for parameters of the substituting scheme. We start with the output state and apply a sequence of inverse unitary transformations $\exp(-iyY)$, $\exp(-iuU)$, $\exp(-iVv)$, and $\exp(-iwW)$ on it. At each step some off-diagonal elements of matrix (36) vanish. This allows us to find u, v, w, and y.

In the first step we determine y. We apply the inverse transformation $\exp(-iyY)$ to the output modes and require that this transformation destroys mutual coupling between modes a_{II} and b_{II},

$$\mathbf{A}_{II}=\mathbf{M}_Y(-y)\mathbf{M}_G(z)\mathbf{A}_{\rm in}. \tag{38}$$

Then the noise parameters of the output modes for the input coherent states read

$$\begin{aligned} B_{a,\rm out}&=|M_{G,12}|^2+|M_{G,14}|^2,\\ B_{b,\rm out}&=|M_{G,32}|^2+|M_{G,34}|^2,\\ D_{ab,\rm out}&=M_{G,11}M_{G,32}+M_{G,13}M_{G,34}. \end{aligned} \tag{39}$$

Parameter $D_{ab,\rm out}$ is real here. After inverse transformation (38) we have

$$\begin{aligned} a_{II}&=\cosh y a_{\rm out}-\sinh y b_{\rm out}^{\dagger},\\ b_{II}&=\cosh y b_{\rm out}-\sinh y a_{\rm out}^{\dagger}. \end{aligned} \tag{40}$$

These modes are uncorrelated, which means that $D_{ab,II}=0$ and $\overline{D}_{ab,II}=0$. The first condition yields

$$y=\frac{1}{2}\,\mathrm{arg\,tanh}\,\frac{2D_{ab,\rm out}}{1+B_{a,\rm out}+B_{b,\rm out}}. \tag{41}$$

It is worth emphasizing that this expression was obtained only from $D_{ab,II}=0$. Nevertheless, the matrices have such a structure that, after inverse transformation, both mutual correlations $D_{ab,II}$ and $\overline{D}_{ab,II}$ vanish.

In the second step we use the same strategy to find the parameters u and v. We introduce the matrix

$$\mathbf{M}_{II}=\mathbf{M}_Y(-y)\mathbf{M}_G(z). \tag{42}$$

The inverse transformations lead to

$$\mathbf{A}_I=\mathbf{M}_U(-u)\mathbf{M}_V(-v)\mathbf{M}_{II}\mathbf{A}_{\rm in} \tag{43}$$

and the modes a_I and b_I are in the coherent states. We will need the noise parameters of modes a_{II} and b_{II}:

$$\begin{aligned} B_{a,II}&=|M_{II,12}|^2+|M_{II,14}|^2,\\ C_{a,II}&=M_{II,11}M_{II,12}+M_{II,13}M_{II,14},\\ B_{b,II}&=|M_{II,32}|^2+|M_{II,34}|^2,\\ C_{b,II}&=M_{II,31}M_{II,32}+M_{II,33}M_{II,34}, \end{aligned} \tag{44}$$

and $C_{a,II}$ and $C_{b,II}$ are purely imaginary. Parameters u and v are found from the conditions $C_{a,I}=0$ and $C_{b,I}=0$, respectively, yielding

$$\begin{aligned} u&=\frac{1}{4}\,\mathrm{arg\,tanh}\,\frac{-2iC_{a,II}}{1+2B_{a,II}},\\ v&=\frac{1}{4}\,\mathrm{arg\,tanh}\,\frac{-2iC_{b,II}}{1+2B_{b,II}}. \end{aligned} \tag{45}$$

Finally we have to determine w. To accomplish this task we calculate the matrix

$$\mathbf{M}_I=\mathbf{M}_U(-u)\mathbf{M}_V(-v)\mathbf{M}_{II}. \tag{46}$$

This matrix is identical with $\mathbf{M}_W(w)$,

$$\mathbf{M}_I=\mathbf{M}_W(w). \tag{47}$$

Thus we can write

$$\cos w=M_{I,11},\quad \sin w=-iM_{I,13}. \tag{48}$$

These two equations determine w uniquely within the interval $[-\pi,\pi]$. We emphasize again that analytical expressions for elements of the matrix $\mathbf{M}_G(z)$ exist and the above given formulas for u, v, w, and y form an analytical solution of the system (35). We do not write down explicit expressions for the parameters as functions of z because the formulas are very lengthy and complicated. For numerical calculations, the above given scheme has been directly adopted.

III. GENERATION OF NONCLASSICAL LIGHT IN NONLINEAR COUPLERS

We assume that a coherent light is fed to the input of the coupler. The coherent input light is a feasible and natural choice. First we discuss the generation of squeezed light and then we address sub-Poissonian light generation.

A. Light squeezing in nonlinear couplers

Let us begin with some general remarks. Since we assume that the input state is the two-mode coherent state $|\xi_a,\xi_b\rangle$, the output state is a pure Gaussian state, created via some symplectic transformation from the input state. The light is squeezed when a variance of some quadrature component is below the level of vacuum fluctuations. This definition can be applied to both single- and multimode fields. For an N-mode field, the quadrature X reads

$$X=\frac{1}{\sqrt{2}}[A+A^{\dagger}], \tag{49}$$

where

$$A=\sum_{j=1}^{N} c_j a_j, \tag{50}$$

and c_j are arbitrary complex numbers fulfilling

$$\sum_{j=1}^{N}|c_j|^2=1, \tag{51}$$

which ensures validity of the commutation relation $[A,A^\dagger]=1$. One can calculate the variances $\langle(\Delta X)^2\rangle$ of all quadratures X and select the lowest variance. If this variance is lower than the coherent state value 1/2, then the light is squeezed. This general definition of multimode squeezing was proposed in [23]. Squeezing defined in such a way is invariant under transformations from the compact group $U(N)$, because the class of all $\{c_j\}$ fulfilling the normalization condition (51) does not change under the $U(N)$ transformations.

The squeezing fully determines whether a Gaussian state is nonclassical or not. All nonclassical Gaussian states are squeezed states. The lowest variance can be called the generalized squeeze variance η and it can be found as a lowest eigenvalue of the correlation matrix $\mathbf{S}$ [23,12]. Multimode squeezing can be measured with the use of multimode homodyne detection; then the complex amplitudes of strong local oscillators play a role of coefficients c_j [12]. In our case modes a and b have the same frequency and one local oscillator is sufficient. The unitary transformations leading to various superpositions (50) can be achieved by passive optical elements. This approach allows us to measure η and it can be extended to multimode optical homodyne tomography with one local oscillator [30,31], because the quantum state of the multimode field is fully determined by the measured quadrature distributions $w[X(c_1,c_2,\ldots,c_N)]$.

For the pure Gaussian state it holds that if η_j is an eigenvalue of $\mathbf{S}$, then also $1/(4\eta_j)$ is an eigenvalue of $\mathbf{S}$ [32]. In our case we deal with four eigenvalues η_1, $1/(4\eta_1)$, η_2, and $1/(4\eta_2)$. The generalized squeeze variance η is the lowest of the eigenvalues,

$$\eta=\min\left\{\eta_1,\frac{1}{4\eta_1},\eta_2,\frac{1}{4\eta_2}\right\}. \tag{52}$$

The light is squeezed for $\eta<1/2$. The sum of the eigenvalues is the trace $\mathrm{Tr}\,\mathbf{S}$,

$$\sum_{j=1,2}\left(\eta_j+\frac{1}{4\eta_j}\right)=\mathrm{Tr}\,\mathbf{S}=2+2B_a+2B_b. \tag{53}$$

The sum of the squares of the eigenvalues is $\mathrm{Tr}\,\mathbf{S}^2$,

$$\sum_{j=1,2}\left(\eta_j^2+\frac{1}{16\eta_j^2}\right)=\sum_{j=1,2}\left(\eta_j+\frac{1}{4\eta_j}\right)^2-1=\mathrm{Tr}\,\mathbf{S}^2. \tag{54}$$

The eigenvalues can be determined from Eqs. (53) and (54). After some algebra, one arrives at the expression for the generalized squeeze variance,

$$\eta=\frac{1}{2}(\chi-\sqrt{\chi^2-1}), \tag{55}$$

where

$$\chi=\frac{1}{2}\{\mathrm{Tr}\,\mathbf{S}+[2(\mathrm{Tr}\,\mathbf{S}^2+1)-(\mathrm{Tr}\,\mathbf{S})^2]^{1/2}\}.$$

It holds that $\chi\geqslant 1$ and $\eta\leqslant 1/2$. We emphasize that the formula (55) is valid only for pure Gaussian states. For a given $\mathrm{Tr}\,\mathbf{S}$ the squeezing will be weakest if $\eta_1=\eta_2$. Inserting this into the above equations, we get a simple estimation for the generalized squeeze variance,

$$\eta_{\mathrm{est}}=\frac{1}{2}+\frac{\langle n_S\rangle}{2}-\frac{1}{2}[(\langle n_S\rangle+1)^2-1]^{1/2}; \tag{56}$$

here

$$\langle n_S\rangle=B_a+B_b, \tag{57}$$

which represents in our case a total number of photons created by spontaneous down-conversion in the coupler. These photons occur in correlated pairs and enhance the squeezing. The formula (56) gives a lower estimate of the squeezing, $\eta\leqslant\eta_{\mathrm{est}}$; the actual squeezing can be stronger than that predicted by Eq. (56). The squeezing increases (i.e., variance η decreases towards zero) with increasing $\langle n_S\rangle$. We can conclude that the nonlinear coupler always generates squeezed light from the coherent input. However, to observe maximum squeezing inherent to the output state, one must measure a variance of an appropriate quadrature,

$$X_{ab}=\frac{1}{\sqrt{2}}[c_a a+c_b b+\mathrm{H.c.}]. \tag{58}$$

How strong can squeezing be generated in the coupler? In the codirectional coupler, $\langle n_S\rangle$ approximately exponentially increases during the propagation,

$$\langle n_S\rangle\approx\exp(2\Lambda_R z); \tag{59}$$

here Λ_R is the largest value among the positive real parts of the eigenvalues (34). For strong parametric amplification (high $\langle n_S\rangle$), Eq. (56) yields

$$\eta\approx\frac{1}{4\langle n_S\rangle}\approx\frac{1}{4}\exp(-2\Lambda_R z). \tag{60}$$

An example of light squeezing in the coupler is given in Fig. 3. An exponential decrease of variance η is modulated by oscillations originating from linear coupling between modes a and b.

B. Sub-Poissonian light generation

Let us consider a general case of the N-mode field in a Gaussian state. The total photon number is

$$n=\sum_{j=1}^{N}n_j=\sum_{j=1}^{N}a_j^\dagger a_j, \tag{61}$$

where a_j is the annihilation operator of the jth mode. The light is sub-Poissonian if the variance $\langle(\Delta n)^2\rangle$ is lower than the mean $\langle n\rangle$. Thus the normally ordered variance

$$V=\langle:(\Delta n)^2:\rangle=\langle(\Delta n)^2\rangle-\langle n\rangle \tag{62}$$

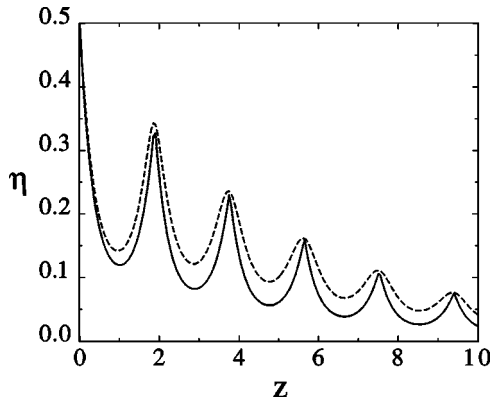

FIG. 3. Squeezing of light in the codirectional coupler. This spatial evolution of generalized squeeze variance η (solid line) was obtained for $g_a=0.6$, $g_b=0.5$, and $\kappa=2$; both modes are initially in a coherent state. The dashed line shows an estimation $\eta_{\rm est}$ based on formula (56). In this and all following figures, relative dimensionless units are used for the coupling constants g_a, g_b, and κ and for the distance z.

is negative for sub-Poissonian light. The variance of any Gaussian state can be expressed in terms of complex amplitudes ξ_j and correlations of fluctuations B_j, C_j, D_{jk}, and $\overline{D}_{jk}$. We decompose operators a_j into $a_j=\Delta a_j+\xi_j$ and we write Δn as

$$\Delta n=\sum_{j=1}^{N}(\Delta a_j^{\dagger}\Delta a_j-B_j)+A+A^{\dagger}; \tag{63}$$

here

$$A=\sum_{j=1}^{N}\xi_j^{*}\Delta a_j. \tag{64}$$

Notice the similarity with Eq. (50). Inserting Eq. (63) into Eq. (62), we have

$$V=\sum_{j\neq k=1}^{N}(|D_{jk}|^2+|\overline{D}_{jk}|^2)+\sum_{j=1}^{N}(B_j^2+|C_j|^2)$$
$$+\langle(A+A^{\dagger})^2\rangle-\sum_{j=1}^{N}|\xi_j|^2. \tag{65}$$

The only negative term, which can give rise to sub-Poissonian statistics, is the last one. The necessary condition for $V<0$ reads

$$\langle(A+A^{\dagger})^2\rangle<\sum_{j=1}^{N}|\xi_j|^2. \tag{66}$$

After renormalization, this gives the squeezing condition discussed in the preceding subsection. This is not surprising. If the Gaussian light is not squeezed, then it has classical analogue and cannot exhibit sub-Poissonian statistics. The variance V depends on ξ_j. The lowest possible value of $\langle(A+A^{\dagger})^2\rangle$ is determined by the generalized squeeze variance η,

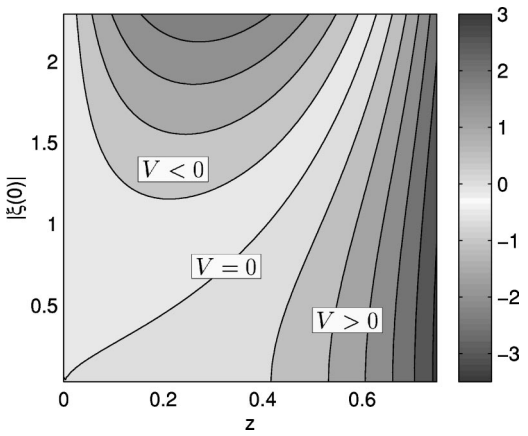

FIG. 4. Sum photon number variance V for different initial complex amplitudes $\xi_a(0)=\xi_b(0)=|\xi(0)|\exp(i\pi/4)$. Both modes are initially in coherent states. The coupling parameters are $g_a=g_b=0.5$ and $\kappa=0.25$. The region of sub-Poissonian light ($V<0$) becomes larger with increasing $|\xi(0)|$.

$$\langle(A+A^{\dagger})^2\rangle\geqslant 2\,\eta\sum_{j=1}^{N}|\xi_j|^2. \tag{67}$$

Inserting this into Eq. (65), we have

$$V_{\rm min}=\sum_{j\neq k=1}^{N}(|D_{jk}|^2+|\overline{D}_{jk}|^2)+\sum_{j=1}^{N}(B_j^2+|C_j|^2)$$
$$-(1-2\,\eta)\sum_{j=1}^{N}|\xi_j|^2. \tag{68}$$

The last term is negative for squeezed states.

Now we can return to the generation of sub-Poissonian light in nonlinear couplers. The input coherent state evolves into the pure squeezed Gaussian state. The complex amplitudes $\xi_j(z)$ depend linearly on inputs $\xi_j(0)$ and we can reach any required $\xi_j(z)$ if we suitably choose the input coherent state $|\xi_a(0),\xi_b(0)\rangle$. Thus we can, in principle, generate sub-Poissonian light at any distance z simply by choosing the input state in such a manner that $\xi_j(z)$ will minimize $\langle(A+A^{\dagger})^2\rangle$ and will be large enough to overcome the positive terms in Eq. (68). For a given input, however, both correlations and complex amplitudes are amplified. The positive terms in Eq. (68) increase as $\exp(4\Lambda_R z)$ while the negative term increases only as $\exp(2\Lambda_R z)$. Finally, the amplified quantum noise prevails and the light becomes super-Poissonian for long z even if the sub-Poissonian region has been reached for small z. Such a behavior has been indeed obtained in [4,6] and we illustrate it in Fig. 4.

IV. DISCUSSION ON THE CODIRECTIONAL COUPLER

In this section we present a discussion on the codirectional coupler. We distinguish between various regimes of the coupler operation which were listed in connection with formula (34) for eigenvalues λ_j.

We start from the subthreshold regime. The z-dependent parameters u, v, w, and y are shown in Fig. 5. We have

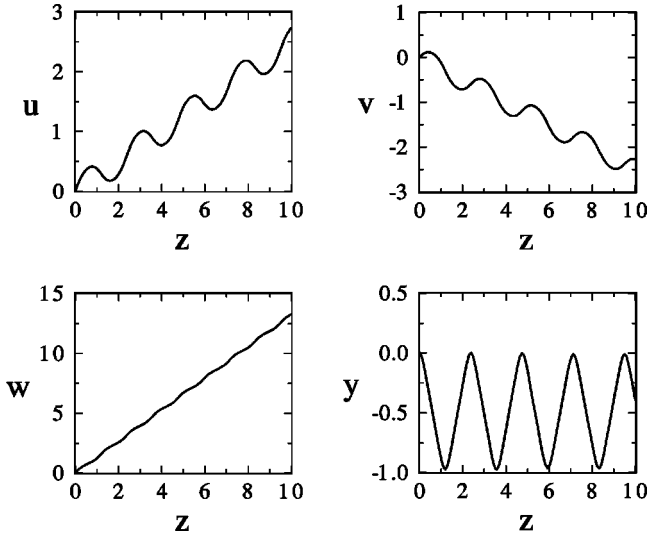

FIG. 5. Parameters of substituting scheme for codirectional coupler below the threshold; $g_a=1$, $g_b=0.5$, and $\kappa=2$.

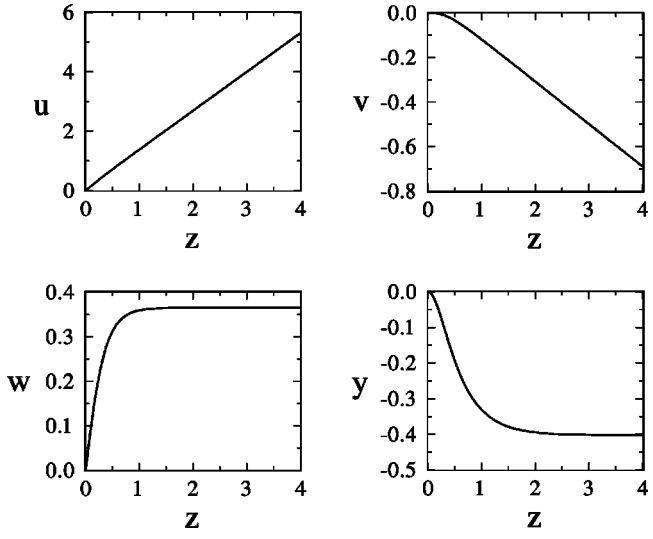

FIG. 6. Parameters of substituting scheme for codirectional coupler above the threshold; $g_a=1.5$, $g_b=0$, and $\kappa=1$.

chosen that $|g_a|\neq|g_b|$ in Fig. 5. Nevertheless, the slopes of an average linear increase (or decrease) of u and v have the same absolute value $|g_a-g_b|/2$, which corresponds to the real part of the subthreshold eigenvalues λ_j, Eq. (34). This symmetry is a consequence of strong linear coupling in the subthreshold regime, which ensures that both modes benefit almost equally from amplification in the first and second waveguides of the coupler. Taking into account Eq. (22), we can express the average linear z dependence of u and v as

$$u\approx\frac{1}{2}(g_a-g_b)z, \quad v\approx\frac{1}{2}(g_b-g_a)z. \tag{69}$$

The linear increase of w is related to the imaginary part of λ_j, and reads $w\approx z\kappa[1-(g_a+g_b)^2/\kappa^2]^{1/2}$. The two-mode squeeze parameter y exhibits a substantially different behavior in that it oscillates periodically. Making use of the differential equations (23), one can find a useful relation between u_+ and y:

$$\kappa\cosh(2y)+(g_a+g_b)\sinh(2y)=\frac{\kappa}{\cosh(4u_+)}. \tag{70}$$

It is clear from Eq. (70) that y is bound for all z, unless $|\kappa|=|g_a+g_b|$.

In the substituting scheme, the main part of the parametric amplification takes place in DOPAs. This reflects that only degenerate parametric processes occur in the coupler. NDOPA mixes the amplified beams. Though this mixing does not significantly contribute to the amplification, it strongly affects the output. The role of NDOPA can be understood as follows. In each waveguide of the coupler, degenerate parametric downconversion creates pairs of correlated photons. Due to the linear coupling, one of the photons can be transferred to the second waveguide, but the quantum correlations between these two photons remain unchanged. This two-step process creates pairs of entangled photons in the modes a and b and it leads to the presence of NDOPA in the substituting scheme.

The distances where $y=0$ deserve special attention. Let us assume a two-mode coherent state at the input. If $y=0$, then we have single-mode squeezed states in modes a, b at the output and these two modes are not correlated. This situation appears periodically for certain lengths of the coupler and is typical for subthreshold operation. When $|y|$ increases, the nonlinear mixing in NDOPA becomes important. This mixing introduces additional noise in the single modes a and b compensated by the correlations between a and b. Though the two-mode field remains in the pure Gaussian state, the single modes are in mixed states. Thus the NDOPA suppresses single-mode squeezing of separate modes a and b. In Sec. III we have introduced the quadrature X_{ab} exhibiting the strongest squeezing. As a rule, this quadrature changes with increasing $|y|$ from the single-mode quadrature towards the two-mode quadrature with almost equal contributions from the modes a and b.

The difference between the exact z dependence of u,v,w and a linear behavior is particularly strong around the threshold. When the coupler is at the threshold and $g_a=g_b=\pm\kappa/2$, all four eigenvalues λ_j are zero and $\mathbf{M}_G(z)\equiv\exp(i\mathbf{F}z)=\mathbf{E}+i\mathbf{F}z$. In this case, u, v, and y increase (or decrease) logarithmically with z, as can be deduced from the analytical algebraic solution presented in Sec. II C.

The properties of the substituting scheme change radically when the coupler operates above the threshold, see Fig. 6. Asymptotically, the single-mode squeeze parameters u and v increase linearly with z while w and y reach some finite asymptotic values. These asymptotic values can be found by a tedious analysis of the algebraic formulas from Sec. II C. It is, however, much more convenient to employ the differential equations (22), (23), and (25) derived in Sec. II B. Taking the limits for $z\to\infty$,

$$|\coth(4u_+)|\to1, \quad y'\to0, \quad w'\to0, \tag{71}$$

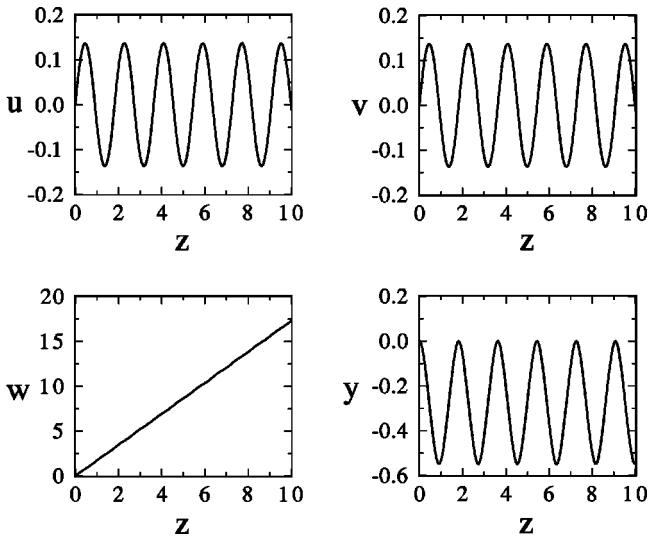

FIG. 7. Parameters of substituting scheme for symmetric codirectional coupler below the threshold; $g_a=0.5$, $g_b=0.5$, and $\kappa=2$.

we obtain from Eqs. (22), (23), and (25)

$$u'_{\rm as}=\frac{g_a-g_b}{2}+\frac{g_a+g_b}{2}\left[1-\left(\frac{\kappa}{g_a+g_b}\right)^2\right]^{1/2},$$

$$v'_{\rm as}=\frac{g_b-g_a}{2}+\frac{g_b+g_a}{2}\left[1-\left(\frac{\kappa}{g_b+g_a}\right)^2\right]^{1/2},$$

$$w_{\rm as}=\frac{1}{2}\arcsin\left(\frac{\kappa}{|g_a+g_b|}\right), \tag{72}$$

$$y_{\rm as}=-\frac{1}{2}\,\mathrm{arg\,tanh}\left(\frac{\kappa}{g_a+g_b}\right);$$

the primes again denote derivatives with respect to z. It is worth noting that the formula for $y_{\rm as}$ can be found only from Eq. (23). Similarly, Eq. (25) is necessary to determine $w_{\rm as}$.

Notice that the slopes $\pm 2u'_{\rm as}$ and $\pm 2v'_{\rm as}$ are just the eigenvalues λ_j of the matrix $i\mathbf{F}$. Above the threshold, the nonlinear interaction locks the signal in the waveguide where it was injected and it suppresses linear coupling with the second waveguide. The modes a and b do not benefit equally from amplification in both waveguides and the slopes $u'_{\rm as}$ and $v'_{\rm as}$ differ when $g_a\neq g_b$. The asymptotic values of $w_{\rm as}$ and $y_{\rm as}$ decrease with increasing ratio $|g_a+g_b|/|\kappa|$ and, eventually, they can become very small. High above the threshold, $u\approx g_a z$, $v\approx g_b z$, $\kappa\approx 0$, $y\approx 0$, and the coupler behaves like two independent DOPAs.

We conclude with some remarks on two special dynamical regimes of the coupler. The exponential amplification completely disappears when $g_a=g_b=g$ and $|g|<|\kappa|/2$. In this case, all four eigenvalues (34) are purely imaginary. As illustrated in Fig. 7, u and v periodically oscillate similarly to y. Since $g_a=g_b$, it holds that $u(z)=v(z)$ as follows from Eq. (22). The substituting scheme reflects the symmetry between the first and second waveguides of the coupler. It is worth noting that $u(z)\equiv v(z)$ oscillate between negative and positive values. For certain lengths z, $u(z)\equiv v(z)=0$ and the coupler can be represented by a simple sequence of beam splitter and NDOPA. Assuming a coherent state at the input of such a coupler, we have the two-mode squeezed state at the output.

Finally, we comment on the case when $g_a=-g_b=g$. The eigenvalues λ_j are complex, $\lambda_j=\pm g\pm i\kappa$, and the coupler is below the threshold. The opposite signs of nonlinear coupling constants result in a kind of decorrelation between modes a and b. The analytical expressions for the parameters (12) take on very simple form

$$u(z)=gz,\quad w(z)=\kappa z,$$
$$v(z)=-gz,\quad y(z)=0. \tag{73}$$

Since $y(z)=0$ for all z, the coupler is equivalent to the sequence of a beam splitter and two DOPAs. This property was already found for other values of coupling constants g_a, g_b, and κ, but only as a special case for certain distances z. In this special configuration, the above feature holds for all z.

V. CONTRADIRECTIONAL COUPLER

In this section we apply the substituting scheme approach to the nonlinear contradirectional coupler of the length L. In the contradirectional coupler, the modes a and b propagate in opposite directions. A degenerate parametric down-conversion takes place in one or both waveguides and the modes a and b are linearly coupled. A nonzero linear coupling between the counterpropagating modes can be achieved by means of distributed feedback grating created in the coupler [17,18], which leads to spatial modulation of the linear coupling parameter κ. The strong phase mismatch $\Delta\beta=\beta_a+\beta_b$ (both propagation constants are positive, $\beta_j>0$) is compensated by the grating whose spatial period is $\Lambda=2\pi/\Delta\beta$.

We use the same notation for the coupling constants as before and we assume again that these constants are all real. The input-output transformation of a nonlinear contradirectional coupler can be determined in three steps. We begin with Heisenberg equations of motion (2) following from momentum operator (1). We assume that the mode b propagates backward, thus we change the sign of the derivative

$$\frac{db}{dz}\to-\frac{db}{dz} \tag{74}$$

in the Heisenberg equations (2) and we obtain new equations of motion. Notice that these equations cannot be obtained from a Hermitian momentum operator. Upon solving the modified Heisenberg equations, we find expressions for $a(L)$ and $b(L)$ as linear combinations of $a(0)$, $a^\dagger(0)$, $b(0)$, and $b^\dagger(0)$. The operators $a(L)$ and $b(L)$ do not fulfill standard commutation relations because the evolution following from the modified Heisenberg equations of motion is not unitary. We must apply proper boundary conditions to retain correct commutation relations. The inputs of the coupler are $a(0)$ and $b(L)$ and the outputs are $a(L)$ and $b(0)$. The latter can

be expressed in terms of the former and thus we arrive at an input-output transformation realized by the nonlinear contradirectional coupler. It was proven in [19] that this transformation is unitary provided that the Heisenberg equations of motion are linear.

The input-output transformation belongs to the same class of symplectic transformations as the input-output transformations realized by the nonlinear codirectional coupler. Particularly, when all coupling constants are real, we can restrict ourselves to the four-parametric subgroup of the group $Sp(4,R)$ and the substituting scheme for the contradirectional coupler is exactly the scheme shown in Fig. 2. However, the dependence of the parameters of the substituting scheme on the length of the coupler and on the values of the coupling constants strongly differs from what we have obtained for the codirectional coupler.

The parameters (12) can be determined in a manner described in Sec. II. The application of the analytical solution as described in Sec. II C is straightforward. The matrix $\mathbf{M}(L)$ can be derived according to the above given prescription and the analytical expressions for its elements can be found in Refs. [5,6]. We address the differential equation approach here in some detail. It should be noted that we have the unitary input-output operator $\mathcal{I}(L)$ for the contradirectional coupler in the form of matrix $\mathbf{M}(L)$. We must replace all operators by corresponding matrices in Eqs. (10) and (15). If we multiply Eq. (15) from the right by the inverse operator $\mathbf{M}^{-1}(L)$, the left-hand side of this equation takes the form

$$\left[\frac{d}{dL}\mathbf{M}(L)\right]\mathbf{M}^{-1}(L)=i[\tilde{g}_a(L)\mathbf{U}+\tilde{g}_b(L)\mathbf{V}+\tilde{\kappa}(L)\mathbf{W}+\tilde{g}_{ab}(L)\mathbf{Y}], \tag{75}$$

where **U**, **V**, **W**, and **Y** denote matrix representations of the operators U, V, W, and Y, respectively. The matrix **X** for any operator X is constructed as

$$\mathbf{X}=\frac{1}{i}\frac{d}{dx}\mathbf{M}_X(x)\bigg|_{x=0}. \tag{76}$$

The coupling parameters $\tilde{g}_a(L)$, $\tilde{g}_b(L)$, $\tilde{\kappa}(L)$, and $\tilde{g}_{ab}(L)$ can be determined from Eq. (75). It was shown in [20] that a wide variety of contradirectional devices can be simulated by codirectional devices, provided that the coupling parameters of simulating codirectional device vary with distance according to Eq. (75).

Having found the coupling parameters, we can write down the differential equations for parameters u, v, w, and y. The system of equations is very similar to Eqs. (22) and (23),

$$\frac{du_-}{dL}=\tilde{g}_-(L) \tag{77}$$

and

$$\mathbf{N}_{\text{right}}\frac{d\mathbf{P}}{dL}=\tilde{\mathbf{C}}, \tag{78}$$

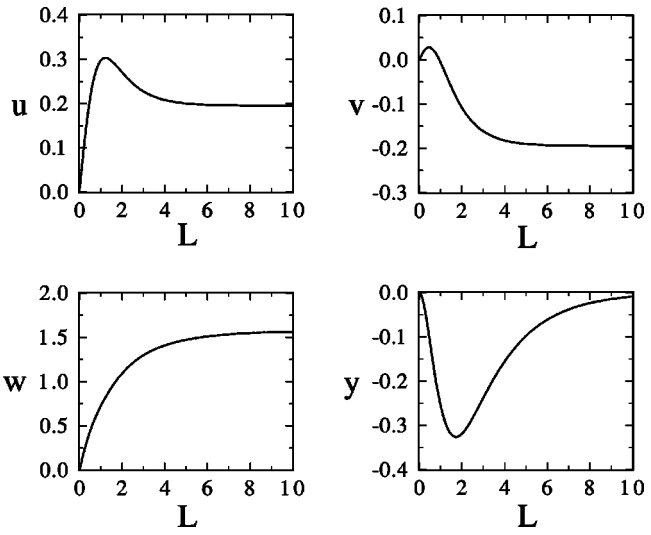

FIG. 8. Parameters of substituting scheme for contradirectional coupler below the threshold; $g_a=0.5$, $g_b=0.1$, and $\kappa=1$.

where

$$\tilde{\mathbf{C}}=\begin{pmatrix}\tilde{g}_+(L)\\ \tilde{\kappa}(L)\\ \tilde{g}_{ab}(L)\end{pmatrix} \tag{79}$$

and $\tilde{g}_\pm(L)=[\tilde{g}_a(L)\pm\tilde{g}_b(L)]/2$. Notice the difference: the right-hand sides in Eqs. (77) and (78) become L-dependent. A new coupling parameter $\tilde{g}_{ab}$ characterizes the strength of nondegenerate parametric down-conversion in the codirectional simulating device discussed in [20].

We start our discussion from the eigenvalues corresponding to the modified Heisenberg equations of motion for contradirectional nonlinear coupler,

$$\lambda_j=\pm(g_a+g_b)\pm[\kappa^2+(g_a-g_b)^2]^{1/2}. \tag{80}$$

All four eigenvalues are real. Recall that in the case of the codirectional coupler we identified two basic regimes of the coupler operation, corresponding to four complex or four real eigenvalues. It turns out that the threshold can be defined also for a contradirectional coupler, and the subthreshold and above-threshold regimes of operation are clearly distinguishable. However, the threshold condition differs from that for the codirectional coupler. The threshold is reached when two eigenvalues are zero; then $|g_a+g_b|=[\kappa^2+(g_a-g_b)^2]^{1/2}$ and the threshold condition reads

$$\kappa^2=4g_ag_b. \tag{81}$$

The coupler is below threshold when $\kappa^2>4g_ag_b$ and above threshold when $\kappa^2<4g_ag_b$.

Figure 8 shows the parameters of the substituting scheme when the coupler is below the threshold. We can see that all parameters asymptotically reach some finite value. This asymptotic behavior of the contradirectional coupler is well known in the literature. The analytical expressions for the asymptotic values of parameters are

$$u_{\rm as}=\frac{1}{2}\,\mathrm{arg\,tanh}\,\frac{g_a-g_b}{[\kappa^2+(g_a-g_b)^2]^{1/2}},$$

$$v_{\rm as}=\frac{1}{2}\,\mathrm{arg\,tanh}\,\frac{g_b-g_a}{[\kappa^2+(g_a-g_b)^2]^{1/2}},\tag{82}$$

$$w_{\rm as}=\frac{\pi}{2}\,\frac{\kappa}{|\kappa|},$$

$$y_{\rm as}=0.$$

Several conclusions can be made from Fig. 8 and formulas (82). The nonlinear coupling y between modes a and b is strongest for some finite L, decreases for long L, and eventually vanishes. The linear coupling w increases with L and reaches asymptotic value $\pi/2$, which means that the modes a and b are interchanged at the beam splitter. Thus we have the following simple picture for the asymptotic behavior of the coupler: the input of mode a is fully transferred to the output of mode b and vice versa. Moreover, each mode is squeezed. The squeezing of both modes is the same because the parametric down-conversions in both waveguides equally contribute to the squeezing. We should mention the special case in which $g_a=g_b$. The squeezing parameters asymptotically vanish, $u_{\rm as}=v_{\rm as}=0$, because squeezings in the first and second waveguides cancel each other. The input of the first waveguide is transferred to the output of the second waveguide without any change, only with phase shift $\pm\pi/2$ (depending on the sign of κ). The same relation holds also for the input of the second waveguide and the output of the first one. The asymptotic behavior of the coupler imposes a limit on the squeezing which can be generated in the coupler from a coherent state input, because the amplification is saturated and reaches some finite asymptotic value. On the other hand, this means that the amplification of noise, discussed in Sec. III B, does not occur here, and the asymptotically sub-Poissonian light can be generated in the coupler [5].

With the help of these results, we can simply explain some phenomena discussed in [5,6]. The authors considered input coherent states or coherent states with superimposed thermal noise. They found that the noise in input mode b suppresses the generation of sub-Poissonian light in mode a for longer coupler lengths L. This result is not surprising in view of our discussion. When the coupler is long enough and it operates below threshold, the output of mode a depends only on the input of mode b. It is thus obvious that the noise in mode b must lead to the suppression of sub-Poissonian light generation at the output of mode a. It was also found in [6] that the output of the coupler can return to the coherent state for long L. This phenomenon appears for the symmetric coupler with $g_a=g_b$. We have shown that for such a coupler the asymptotic transformation is $b(0)=\pm ia(0)$ and $a(L)=\pm ib(L)$. Thus the output coherent state in $a(L)$ is actually an input coherent state in $b(L)$.

The behavior of the contradirectional coupler changes when the threshold is reached. The parameters (12) for the coupler exactly at the threshold are shown in Fig. 9. Notice

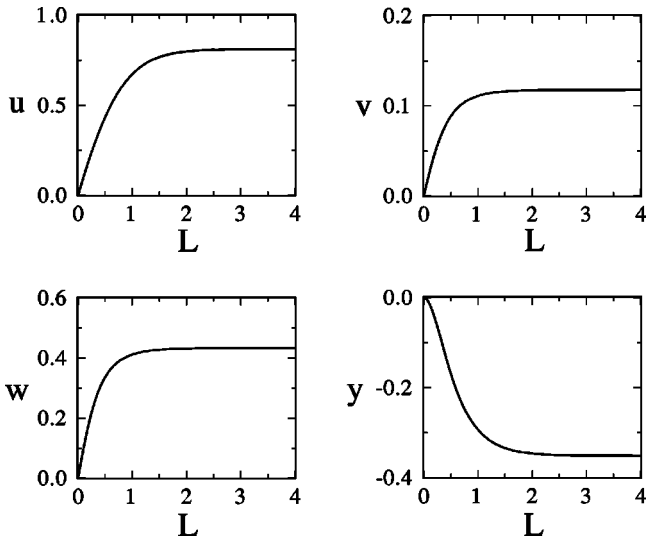

FIG. 9. Parameters of substituting scheme for contradirectional coupler at the threshold; $g_a=1$, $g_b=0.25$, and $\kappa=1$.

that all parameters reach some nonzero asymptotic value and the intermodal coupling is present even for very long L. The analytical expressions for the asymptotic values of the parameters could be found following the approach of Sec. II C and using the asymptotic form of the input-output matrix $\mathbf{M}(L\to\infty)$,

$$\begin{aligned}a_{\rm as}(L)&=\frac{g_a+g_b}{2g_b}a(0)+i\frac{|g_a+g_b|}{2g_b}a^\dagger(0)\\&\quad+i\frac{|g_a+g_b|}{\kappa}b(L)+\frac{g_a-g_b}{\kappa}b^\dagger(L),\\ b_{\rm as}(0)&=i\frac{|g_a+g_b|}{\kappa}a(0)+\frac{g_b-g_a}{\kappa}a^\dagger(0)\\&\quad+\frac{g_a+g_b}{2g_a}b(L)+i\frac{|g_a+g_b|}{2g_a}b^\dagger(L),\end{aligned}\tag{83}$$

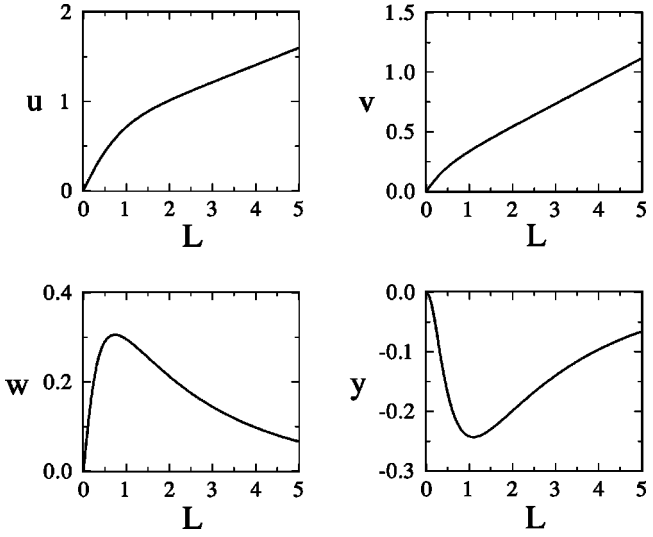

FIG. 10. Parameters of substituting scheme for contradirectional coupler above the threshold; $g_a=1$, $g_b=0.5$, and $\kappa=1$.

where it is assumed that $L \to \infty$ and $\kappa^2 = 4 g_a g_b$ holds.

If we move above the threshold, we can observe that both w and y reach asymptotically zero and the nonlinear coupler behaves like two independent DOPAs, see Fig. 10. The reason for this change of the behavior is that the nonlinear interaction is now strong enough to suppress the transfer from the input of the first waveguide to the output of the second one. Single-mode squeeze parameters asymptotically increase linearly with L according to

$$|u'_{\mathrm{as}}| = |v'_{\mathrm{as}}| = \frac{1}{2}\{|g_a + g_b| - [\kappa^2 + (g_a - g_b)^2]^{1/2}\}. \quad (84)$$

The increase is the same for both modes even if the coupling constants g_a and g_b differ.

VI. CONCLUSIONS

In conclusion, we have considered a substituting scheme for directional and contradirectional nonlinear optical couplers. The scheme represents a unitary transformation realized by the coupler. The advantage of the substituting scheme lies in its relatively simple structure. It is formed by a sequence of beam splitter, two DOPAs, and one NDOPA. Using the group-theoretical approach and considering propagation of the two-mode coherent state through the device, we were able to find analytical expressions for the parameters of the substituting scheme.

We have discussed generation of nonclassical light in the coupler and found that the coupler always generates squeezed light from the input coherent state. We have provided a simple estimation of squeeze variance relating it to the mean number of photons generated by spontaneous down-conversion in the coupler.

We have demonstrated that properties of the substituting scheme clearly reflect various dynamical regimes of the codirectional coupler and we have obtained simple asymptotic formulas for the parameters of the device when the coupler is above the threshold. It was shown that in certain cases the coupler can be replaced by a sequence of beam splitter and two DOPAs or by a combination of a beam splitter and NDOPA.

We have shown that the idea of the substituting scheme is fully applicable also to the contradirectional coupler. We have identified the threshold condition for the contradirectional coupler and adopted the parameters of the substituting scheme to study the behavior of subthreshold and above-threshold regimes of operation. Some results obtained earlier were simply explained.

ACKNOWLEDGMENTS

This work was partly supported by Grant No. VS96028 and Research Project CEZ: J14/98: 15100009 ''Wave and Particle Optics'' of the Czech Ministry of Education and by Grant No. 202/00/0142 of the Czech Grant Agency.

[1] G. Assanto, A. Laureti-Palma, C. Sibilia, and M. Bertolotti, Opt. Commun. **110**, 599 (1994).
[2] J. Janszky, C. Sibilia, M. Bertolotti, P. Adam, and A. Petak, Quantum Semiclassic. Opt. **7**, 509 (1995).
[3] H. Hatami-Hanza and P.L. Chu, Opt. Commun. **124**, 90 (1996).
[4] J. Peřina and J. Peřina, Jr., Quantum Semiclassic. Opt. **7**, 541 (1995).
[5] J. Peřina and J. Peřina, Jr., Quantum Semiclassic. Opt. **7**, 849 (1995).
[6] J. Peřina and J. Peřina, Jr., J. Mod. Opt. **43**, 1951 (1996).
[7] N. Korolkova and J. Peřina, Opt. Commun. **137**, 263 (1997).
[8] A. Chefles and S.M. Barnett, J. Mod. Opt. **43**, 709 (1996).
[9] N. Korolkova and J. Peřina, Opt. Commun. **136**, 135 (1997).
[10] J. Peřina, Jr. and J. Peřina, Quantum Semiclassic. Opt. **9**, 443 (1997).
[11] J. Fiurášek and J. Peřina, J. Mod. Opt. **46**, 1255 (1999).
[12] J. Fiurášek and J. Peřina, J. Opt. B: Quantum Semiclassical Opt. **2**, 10 (2000).
[13] J. Janszky, A. Petak, C. Sibilia, M. Bertolotti, and P. Adam, Quantum Semiclassic. Opt. **7**, 145 (1995).
[14] L. Mišta, Jr., J. Řeháček, and J. Peřina, J. Mod. Opt. **45**, 2269 (1998).
[15] J. Fiurášek, J. Křepelka, and J. Peřina, Opt. Commun. **167**, 115 (1999).
[16] J. Peřina, Jr. and J. Peřina, in Progress in Optics, edited by E. Wolf (Elsevier, Amsterdam, in press).
[17] D. Campi, C. Coriasso, A. Stano, L. Faustini, C. Cacciatore, C. Rigo, and G. Meneghini, Appl. Phys. Lett. **72**, 537 (1998).
[18] C. Coriasso, D. Campi, L. Faustini, A. Stano, and C. Cacciatore, IEEE J. Quantum Electron. **35**, 298 (1999).
[19] A. Luis and J. Peřina, Quantum Semiclassic. Opt. **8**, 39 (1996).
[20] J. Řeháček, L. Mišta, Jr., and J. Peřina, J. Mod. Opt. **46**, 801 (1999).
[21] G.J. Milburn, J. Phys. A **17**, 737 (1984).
[22] R. Simon, E.C.G. Sudarshan, and N. Mukunda, Phys. Rev. A **37**, 3028 (1988).
[23] R. Simon, N. Mukunda, and B. Dutta, Phys. Rev. A **49**, 1567 (1994).
[24] E.C.G. Sudarshan, Ch.B. Chiu, and G. Bhamathi, Phys. Rev. A **52**, 43 (1995).
[25] Arvind, B. Dutta, N. Mukunda, and R. Simon, Phys. Rev. A **52**, 1609 (1995).
[26] A. Luis and L.L. Sánchez-Soto, Quantum Semiclassic. Opt. **7**, 153 (1995).
[27] S.K. Hong, Ch.I. Um, K.H. Yeon, and D.H. Kim, J. Opt. B: Quantum Semiclassical Opt. **1**, 571 (1999).
[28] B.C. Sanders and D.A. Rice, Phys. Rev. A **61**, 013805 (2000).
[29] J. Wei and E. Norman, J. Math. Phys. **4**, 575 (1963).
[30] G.M. D'Ariano, M.F. Sacchi, and P. Kumar, Phys. Rev. A **61**, 013806 (2000).
[31] M.G. Raymer and A.C. Funk, Phys. Rev. A **61**, 015801 (2000).
[32] M. Kitamura and T. Tokihiro, J. Opt. B: Quantum Semiclassical Opt. **1**, 546 (1999).